Determination of gap defect states in organic bulk heterojunction solar cells from capacitance measurements

Pablo P. Boix,[1] Germà Garcia-Belmonte,[1,a)] Udane Muñecas,[2] Marios Neophytou,[2,b)] Christoph Waldauf,[2] and Roberto Pacios[2]

[1]*Departament de Física, Photovoltaic and Optoelectronic Devices Group, Universitat Jaume I, Castelló ES-12071, Spain*

[2]*Department of Microsystems, IKERLAN-IK4 S. Coop., P° J M Arizmendiarrieta, 2. 20500 Arrasate-Mondragón, Gipuzkoa, Spain*

(Received 28 July 2009; accepted 10 November 2009; published online 7 December 2009)

Energy distributions [density-of-states (DOS)] of defects in the effective band gap of organic bulk heterojunctions are determined by means of capacitance methods. The technique consists of calculating the junction capacitance derivative with respect to the angular frequency of the small voltage perturbation applied to thin film poly(3-hexylthiophene) (P3HT) [6,6]-phenyl C_{61}-butyric acid methyl ester (PCBM) solar cells. The analysis, which was performed on blends of different composition, reveals the presence of defect bands exhibiting Gaussian shape located at $E \approx 0.38$ eV above the highest occupied molecular orbital level of the P3HT. The disorder parameter σ, which accounts for the broadening of the Gaussian DOS, lies within the range of 49–66 meV. The total density of defects results of order 10^{16} cm^{-3}. © *2009 American Institute of Physics*. [doi:10.1063/1.3270105]

Bulk heterojunctions formed by an interpenetrating blend of an optically active polymer and electron accepting molecules constitute a very promising route toward cheap and versatile solar cells.[1,2] The combination of poly(3-hexylthiophene) (P3HT) and [6,6]-phenyl C_{61}-butyric acid methyl ester (PCBM) in organic blends has recently shown high photovoltaic performance approaching 5% energy-conversion efficiency.[3] In order to further improve organic solar cell performance extracting information about defect states and their role as trapping or recombination centers seems to be crucial. It is well known that P3HT is a conjugated polymer that in exposure to oxygen and/or moisture results *p*-doped.[4–6] Under such conditions, it has been suggested that the P3HT-aluminum contact shows a Schottky diode behavior: band bending with a corresponding depletion zone formed at the cathode contact[7,8] due to the presence of acceptor defects. Capacitance measurements usually exhibit a Mott–Schottky characteristics ($C^{-2} \propto V$),[8–10] which can be readily interpreted as a strong indication of the presence of acceptor levels within the P3HT energy gap. Information about bulk defect states in polymer-fullerene solar cells has been extracted from subgap optical absorption experiments,[11] low excitation intensity transient absorption spectroscopy,[12] and thermally stimulated current techniques.[13]

Defect states might have detrimental effects on the solar cells performance.[13] Charged defects within the gap alter the electrical field profile and might reduce the drift driving force for carrier transport, and consequently diminish carrier collection at the contacts. In extreme cases, the electrical field can be even suppressed in a significant portion of the active layer.[14] As usually admitted in the case of *a*-Si and other thin-film *p-i-n* solar cell structures, the presence of impurities in a high enough concentration lies behind the cell performance degradation.[15]

This work further investigates the density and energetics of defect states within the gap of P3HT, and explores the effect of PCBM molecules in blends of different composition. The study is performed by analyzing capacitance dependences on both bias voltage $C(V)$ and frequency $C(f)$ of complete cells, following known techniques for characterizing semiconductor contact effects.[16–18]

Standard organic solar cells comprising the following vertical structure ITO/PEDOT:PSS(40 nm)/P3HT:PCBM (150 nm)/Ca(10 nm)/Ag(200 nm) were prepared using chlorobenzene as the solvent for both materials P3HT (from Rieke Materials) and PCBM (from Nano-C). The weight ratio between P3HT and PCBM in the blend was varied in order to verify the influence of the PCBM amount in the defect states distribution. The resulting devices were then thermally annealed at 140 °C for 15 min. Finally, all the substrates were encapsulated with an epoxy resin and glass, taking special care to leave at least 2 mm from the diode to the encapsulating glass to prevent any oxygen/moisture penetration from the edges.

The capacitance measurements were performed with an Autolab PGSTAT-30 equipped with a frequency analyzer module. AC oscillating amplitude was as low as 20 mV (rms) to maintain the linearity of the response. Measurements were performed at zero bias for $C(f)$ analysis, and at 100 Hz for $C(V)$ analysis, always in dark conditions and room temperature. Photovoltaic response was observed to result in conversion efficiencies around 3.5%.

Defect states within the band gap contribute to the junction capacitance depending on their energy and space position. If the angular frequency of the perturbation is low enough so that all states can follow the ac signal, the capacitance reflects the energy density of defect states (DOS) $g_t(E)$ at a certain position in the depletion region. Such a position

[a)]Author to whom correspondence should be addressed. Electronic mail: garciag@uji.es. Tel.: +34 964 728040. FAX: +34 964 729218.

[b)]Present address: Department of Mechanical Engineering and Materials Science and Engineering, Cyprus University of Technology, 3603 Limassol, Cyprus.

 © 2009 American Institute of Physics

Author complimentary copy. Redistribution subject to AIP license or copyright, see http://apl.aip.org/apl/copyright.jsp

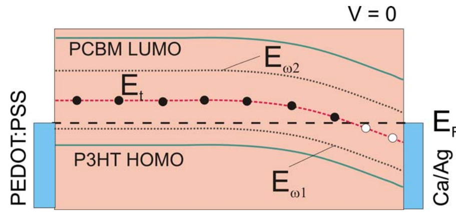

FIG. 1. (Color online) Band diagram of a *p*-doped P3HT:PCBM blend at zero bias voltage. A depletion zone is formed near the cathode. The crossing point between the Fermi level E_F and the defect energy E_t within the depletion zone marks the position of occupancy change. $E_{\omega 1}$ corresponds to a measurement condition at which defects cannot respond to the perturbation because of the high frequency or low temperature. Instead $E_{\omega 2}$ (low frequency or high temperature conditions) is far above the defect energy so that the occupancy is determined by E_F.

is determined by the point at which the Fermi level E_F crosses the defect energy levels (see Fig. 1). This simple assumption gives rise to the following expression:[19]

$$C = q^2 \frac{\tilde{u}_0}{\tilde{u}_{\text{ext}}} g_t(E_F), \tag{1}$$

which informs that only states at the Fermi level efficiently contribute to the capacitance. In Eq. (1), q represents the elementary charge and the ratio $\tilde{u}_0/\tilde{u}_{\text{ext}}$ stands for the drop of the external ac perturbation over the space charge region of the junction. This ratio depends on the junction type and the consequent shape of the electrical field in the depletion zone. If not all defects can follow the perturbation because of high modulation frequencies or low temperatures, only defects below (in case of a *p*-type semiconductor) certain demarcation energy E_ω will be able to contribute to the junction capacitance[20]

$$E_\omega = k_B T \ln\left(\frac{\omega_0}{\omega}\right). \tag{2}$$

Here k_BT corresponds to the thermal energy and ω_0 denotes an attempt-to-escape frequency, which usually lies within the order of 10^{12} s^{-1}, and $\omega = 2\pi f$ the angular frequency of the perturbation. The same concept has been also used in analyzing the transient relaxation of photogenerated charges in organic blends.[21] This demarcation energy marks those defect levels which can be charged and discharged by the ac signal (Fig. 1) then contributing to the measured capacitance. Varying the frequency of the perturbation voltage allows one to establish different demarcation energies according to Eq. (2). Following this approach, the capacitance spectra is viewed as an energy spectroscopy which explores energy levels of faster states at high frequencies [near the (highest occupied molecular orbital) HOMO of the polymer], and sweeps toward midgap as the frequency decreases (slower defects far from the HOMO level), i.e., $E_\omega = E - E_{\text{HOMO}}$. The defect distribution was stated to be related to the derivative of the capacitance with respect to the frequency as[19]

$$g_t(E_\omega) = -\frac{V_{\text{fb}}}{qwk_BT}\frac{dC(\omega)}{d\ln\omega} \tag{3}$$

being w the width of the depletion zone, and V_{fb} is the flat-band potential. Equation (3) was derived assuming the simplified relation $\tilde{u}_0 \approx \tilde{u}_{\text{ext}}$.

We show in Fig. 2(a) the capacitance spectra $C(f)$ obtained at zero bias in the dark at room temperature for different devices. The $C(f)$ curves exhibit an increment of the capacitance toward low frequencies resulting from contributions of defect levels in the gap. In order to verify that the analyzed devices exhibit Mott–Schottky characteristics, it is displayed in Fig. 2(b) the capacitance measured at low frequency (100 Hz) as $C^{-2}(V)$. A linear relationship is observed at low forward voltages, being the intercept with the real axis related to the flat-band potential. The density of defect states n is derived from the slope the by means of the Mott–Schottky relation

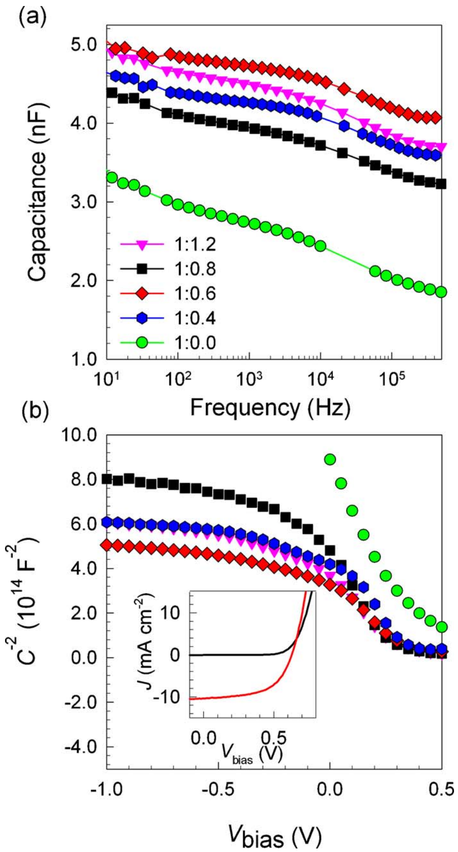

FIG. 2. (Color online) (a) Capacitance spectra measured at zero bias voltage for devices of different blend composition (weight ratio as indicated). (b) Mott–Schottky characteristics $[C^{-2}(V)]$ exhibiting full depletion at reverse bias and a linear relationship [Eq. (4)] at low forward bias (0.0–0.3 V). In the inset: example of current density-voltage characteristics of a cell of P3HT:PCBM of weight ratio (1:0.8).

$$C^{-2} = \frac{2(V_{\text{fb}} - V)}{A^2 q\varepsilon\varepsilon_0 n}, \tag{4}$$

where A corresponds to the device active surface (9 mm^2), ε is the relative dielectric constant of the blend, ε_0 the permittivity of the vacuum, and n the total concentration of acceptor impurities, including the defect density explored from $C(f)$ because the measuring frequency is low-enough to consider their contribution[16] (see Table I). The total density results in $n \approx 3-6 \times 10^{16}$ cm^{-3}.

By applying Eq. (3) to the capacitance spectra in Fig. 2(a), the DOS obtained as a function of $E - E_{\text{HOMO}}$ is plotted in Fig. 3. We have used values for V_{fb} extracted from the Mott–Schottky analysis in Fig. 2(b) and listed in Table I, and assumed that the layers are nearly fully depleted at zero bias. It is observed that high-energy data (low-frequency) are very noisy because of the derivative procedure required. Never-

Author complimentary copy. Redistribution subject to AIP license or copyright, see http://apl.aip.org/apl/copyright.jsp

TABLE I. Fitting results obtained from defect DOS [Eq. (3)] and Mott–Schottky analysis [Eq. (5)] using blends of different weight ratio.

P3HT:PCBM (weight ratio)	n_t (10^{16} cm^{-3})	σ (meV)	E_0 (eV)	V_{fb} (V)	n (10^{16} cm^{-3})
1:0.0	2.1	56	0.39	0.40	3.2
1:0.4	1.5	49	0.38	0.36	5.0
1:0.6	1.5	52	0.38	0.36	6.8
1:0.8	1.2	66	0.38	0.30	4.3
1:1.2	1.7	59	0.38	0.33	6.2

theless the technique allows extracting the DOS shape at midenergies with high-enough resolution. The DOS can be analyzed by regarding a Gaussian shape centered at the maximum of the distribution E_0

$$g_t(E_\omega) = \frac{n_t}{\sqrt{2\pi}\sigma}\exp\left[-\frac{(E_0-E_\omega)^2}{2\sigma^2}\right]. \quad (5)$$

The Gaussian DOS resulting from the fits by using different cells are centered at $E_0=0.38$ eV. The disorder parameter σ, which accounts for the broadening of the Gaussian DOS, lies within the range of 49–66 meV. In good agreement with values found in most cases for conducting polymers $\sigma \approx 0.1$ eV.[22,23] Finally, n_t denotes the density of defects which results in $1-2\times10^{16}$ cm^{-3} (see Table I), in accordance to densities extracted from absorption methods.[12] It should be noted the slight dispersion exhibited by the parameters appearing independent of the blend composition, even for pure P3HT devices. This observation reinforces the idea that the investigated defect states belong to the polymer. To confirm this we also built devices containing only PCBM molecules which did not exhibit at all the behavior reported here. As listed in Table I, the acceptor density extracted from the $C(V)$ analysis results slightly greater than the defect density obtained from $C(f)$, i.e., $n>n_t$. This is because the Mott–Schottky slope includes the effect not only of n_t but also of shallow impurities ($E-E_{HOMO}<0.3$ eV) which are presumably ionized at room temperature.

The origin of the defect states reported here must be found within intrinsic impurities induced during film preparation: vacancies, dangling bonds, or ends of chains. These defects create localized states in the band gap, as usually reported in amorphous semiconductors.[24,25] Defect bands split up into two set of states representing neutral (lower, singly electron occupied) and acceptorlike (higher, double electron occupied) bands. Band broadening is also expected by effect of interactions resulting from the disordered environment in which each molecule is placed. We then conclude that the defect band found in this study might have a great influence on the electrical field profile when charged because of the defect DOS of order 10^{16} cm^{-3}.

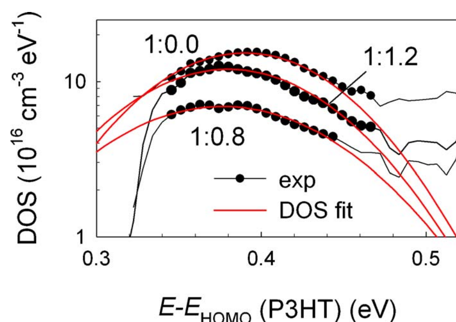

FIG. 3. (Color online) Density of defect states as a function of the energy with respect to the P3HT HOMO level (demarcation energy), $E-E_{HOMO}$, calculated using Eq. (3) and the capacitance spectra in Fig. 1(a). Gaussian DOS fits [Eq. (5)] are also displayed. Composition of the blend is marked in each distribution.

We thank financial support from Ministerio de Educacion y Ciencia under project HOPE Consolider-Ingenio 2010 (Grant No. CSD2007-00007) and Universitat Jaume I (Grant No. P1.1B2008-32). M.N. would like to thank Ikerlan Microsystems for Ph.D. internship funding.

[1] C. J. Brabec, N. S. Sariciftci, and C. Hummelen, Adv. Mater. **11**, 15 (2001).
[2] S. H. Park, A. Roy, S. Beaupré, S. Cho, N. Coates, J. S. Moon, D. Moses, M. Leclerc, K. Lee, and A. J. Heeger, Nat. Photonics **3**, 297 (2009).
[3] W. Ma, C. Yang, X. Gong, K.-S. Lee, and A. J. Heeger, Adv. Funct. Mater. **15**, 1617 (2005).
[4] M. S. A. Abdou, F. P. Orfino, Y. Son, and S. Holdcroft, J. Am. Chem. Soc. **119**, 4518 (1997).
[5] S. Hoshino, M. Yoshida, S. Uemura, T. Kodzasa, N. Takada, T. Kamata, and K. Yase, J. Appl. Phys. **95**, 5088 (2004).
[6] E. J. Meijer, A. V. G. Mangnus, B.-H. Huisman, G. W. 't Hooft, D. M. de Leeuw, and T. M. Klapwijk, Synth. Met. **142**, 53 (2004).
[7] G. Dennler, C. Lungenschmied, N. S. Saricifti, R. Schwödiauer, S. Bauer, and H. Reiss, Appl. Phys. Lett. **87**, 163501 (2005).
[8] G. Garcia-Belmonte, A. Munar, E. M. Barea, J. Bisquert, I. Ugarte, and R. Pacios, Org. Electron. **9**, 847 (2008).
[9] G. Garcia-Belmonte, P. P. Boix, J. Bisquert, M. Sessolo, and H. J. Bolink, "Simulataneous determination of carrier lifetime and electron density-of-states in P3HT:PCBM organic solar cells under illumination by impedance spectroscopy," Sol. Energy Mater. Sol. Cells (in press).
[10] J. Bisquert, G. Garcia-Belmonte, A. Munar, M. Sessolo, A. Soriano, and H. J. Bolink, Chem. Phys. Lett. **465**, 57 (2008).
[11] L. Goris, A. Poruba, L. Hod'áková, M. Vanecek, K. Haenen, M. Nesládek, P. Wagner, D. Vanderzande, L. De Schepper, and J. V. Manca, Appl. Phys. Lett. **88**, 052113 (2006).
[12] A. F. Nogueira, I. Montanari, J. Nelson, J. R. Durrant, C. Winder, N. Z. Sariciftci, and C. Brabec, J. Phys. Chem. B **107**, 1567 (2003).
[13] T. P. Nguyen, Phys. Status Solidi A **205**, 162 (2008).
[14] J. Nelson, *The Physics of Solar Cells* (Imperial College Press, London, 2003).
[15] J. Poortmans and V. Arkhipov, *Thin Film Solar Cells. Fabrication, Characterization, and Applications* (Wiley, Chichester, 2006).
[16] L. C. Kimerling, J. Appl. Phys. **45**, 1839 (1974).
[17] I. Balberg, J. Appl. Phys. **58**, 2603 (1985).
[18] S. S. Hegedus and W. N. Shafarman, Prog. Photovoltaics **12**, 155 (2004).
[19] T. Walter, R. Herberholz, C. Müller, and H. W. Schock, J. Appl. Phys. **80**, 4411 (1996).
[20] S. S. Hegedus and E. A. Fagen, J. Appl. Phys. **71**, 5941 (1992).
[21] T. Moehl, V. G. Kytin, J. Bisquert, M. Kunst, H. J. Bolink, and G. Garcia-Belmonte, ChemSusChem **2**, 314 (2009).
[22] J. Bisquert, G. Garcia-Belmonte, and J. García-Cañadas, J. Chem. Phys. **120**, 6726 (2004).
[23] I. N. Hulea, H. B. Brom, A. J. Houtepen, D. Vanmaekelbergh, J. J. Kelly, and E. A. Meulenkamp, Phys. Rev. Lett. **93**, 166601 (2004).
[24] N. F. Mott and E. A. Davis, *Electronic Processes in Noncrystalline Materials* (Clarendon, Oxford, 1979).
[25] A. Madan and M. P. Shaw, *The Physics and Applications of Amorphous Semiconductors* (Academic, Boston, 1988).

Author complimentary copy. Redistribution subject to AIP license or copyright, see http://apl.aip.org/apl/copyright.jsp